Chemical Geology 608 (2022) 121030

Contents lists available at ScienceDirect

Chemical Geology

journal homepage: www.elsevier.com/locate/chemgeo

Degradation of Hg signals on incipient weathering: Core versus outcrop geochemistry of Upper Permian shales, East Greenland and Mid-Norwegian Shelf

Junhee Park [a,*], Holly J. Stein [a,b], Svetoslav V. Georgiev [a,c], Judith L. Hannah [a,b]

[a] AIRIE Program, Colorado State University, Fort Collins 80523-1482, CO, USA
[b] Institute of Geosciences, University of Oslo, 0316 Oslo, Norway
[c] Geological Institute, Bulgarian Academy of Sciences, Acad. G. Bonchev Bl. 24, 1113 Sofia, Bulgaria

ARTICLE INFO

Editor: Karen Johannesson

Keywords:
Organic-rich shale weathering
Hg signals
Principal component analysis
Late Permian
East Greenland

ABSTRACT

Mercury (Hg) enrichment and elevated ratios of Hg to total organic carbon (Hg/TOC) in sedimentary rocks have often been linked to volcanism from large igneous provinces (LIPs). Primary Hg and TOC contents of sediments can be altered by secondary processes like *extreme* weathering. These effects must be evaluated before tying Hg anomalies in weathered rocks directly to LIP events. However, the effects of *incipient* weathering on Hg contents and Hg/TOC ratios are not known. In this study, we elucidate the behavior of Hg during incipient weathering by investigating visually pristine black shales from outcrops of the Ravnefjeld Formation in East Greenland (GRL) and comparing them to drill core equivalent intervals acquired from the same outcrop area and correlative shales from the mid-Norwegian shelf (MNS). By using geochemical investigations and principal component analysis, we characterize the main host phases of Hg and relate the different Hg contents of pristine samples from GRL and MNS to different Hg inputs during shale deposition. Compared with pristine drill core samples, incipiently weathered outcrop shales have up to 77% lower Hg contents and up to 64% lower Hg/TOC ratios. Incipient weathering causes the early degradation of Hg signals, which masks the primary Hg and Hg/TOC signals in sedimentary rocks. Therefore, we suggest that the presence and effects of weathering in sedimentary rock should be evaluated before discussing Hg signals.

1. Introduction

Large igneous provinces (LIPs) have been regarded as the main trigger of global environmental perturbations or even mass extinctions (e.g., Percival et al., 2015; Shen et al., 2019a). Because volcanic emissions are the largest known source of atmospheric Hg prior to significant anthropogenic inputs, mercury (Hg) concentration or Hg/TOC ratio anomalies in sedimentary rocks are commonly interpreted as tracers of massive volcanism (e.g., Percival et al., 2018; Clapham and Renne, 2019).

Characterization of the input sources of Hg is important for interpreting Hg contents. The size and type of volcanoes and proximity to landmass have been identified as the main factors to affect Hg contents in sedimentary rocks (Percival et al., 2018; Them et al., 2019). Recognition of true anomalies in Hg input requires that Hg concentrations be normalized to total organic carbon (TOC), reported as Hg/TOC ratios because organic matter (OM) is the acclaimed primary host of Hg in sedimentary rocks (e.g., Fitzgerald and Lyons, 1973; Gehrke et al., 2009). Sulfide and clay minerals, however, may also contain significant amounts of Hg. For example, Shen et al. (2020) show that sulfide can be the primary host phase of Hg in sedimentary rocks deposited under strongly euxinic conditions, and Kongchum et al. (2011) report a substantial relationship between Hg contents and the amount of clay minerals in modern sediments. Therefore, understanding depositional settings and the host of Hg in sedimentary rocks are essential for geochemical interpretations.

Measured Hg contents and Hg/TOC ratios in sediments are affected by the post-depositional history of the rock as well as the depositional setting. Charbonnier et al. (2020) investigated the impact of intense weathering on Hg/TOC anomalies compared to relatively pristine samples. Total organic carbon was almost completely removed from their weathered samples and, as a result, Hg/TOC appeared

* Corresponding author.
E-mail addresses: Juni.Park@colostate.edu, Juni.Park@colostate.edu (J. Park).

https://doi.org/10.1016/j.chemgeo.2022.121030
Received 8 March 2022; Received in revised form 8 June 2022; Accepted 20 July 2022
Available online 25 July 2022

anomalously high. This exaggerated Hg/TOC signal can be mistakenly interpreted as an indicator of LIP activity if the oxidation of sedimentary rocks is not considered. Such misinterpretation should be easily avoidable, as extreme weathering can be identified with the naked eye, for example by the color-change in weathered samples (Charbonnier et al., 2020).

The mobility of Hg during incipient weathering has not yet been studied. Unlike extreme weathering, incipient weathering of shale is harder to identify visually, especially in black organic-rich shales (Marynowski et al., 2011; Georgiev et al., 2012; Tuttle et al., 2014; Marynowski et al., 2017) and is usually defined by chemical means. Peng et al. (2004) define "incipient" weathering as oxidation of sulfide, but limited oxidation of OM. It is well-known that sulfide is oxidized rapidly and earlier than the oxidation of OM (Petsch et al., 2000; Wildman et al., 2004). Incipient weathering is known to alter primary elemental contents significantly (e.g., S, Pb, Sc), the oxygen content of OM (oxygen index; OI), and Re-Os isotopic ratios in shale (Georgiev et al., 2012). Significant reductions in TOC, S, Mo, and changes in stable isotope compositions have been reported in partially weathered black shales (e.g., Marynowski et al., 2017). Similarly, any differential mobility of Hg and TOC during incipient weathering has the potential to alter primary Hg/TOC ratios in sedimentary rocks, which may lead to misinterpreted signals. It is essential, therefore, to evaluate Hg behavior during incipient weathering so that the geologic significance of Hg signals and Hg/TOC ratios can be accurately interpreted.

In this study, we report the effects of incipient weathering on Hg contents and Hg/TOC ratios in incipiently weathered organic-rich shale from East Greenland (GRL) outcrops, adjacent correlative pristine drill core, and coeval pristine shale from the mid-Norwegian shelf (MNS) drill core. We discuss the main host phases of Hg and the fate of Hg during and after incipient weathering by using principal component analysis (PCA) and newly acquired Hg concentration data. We suggest incipient weathering plays a pivotal role in the early degradation of Hg contents in sedimentary rocks.

2. Geological settings and samples

The shales of the Upper Permian Ravnefjeld Formation of East Greenland reflect anoxic-euxinic conditions immediately preceding the Permian-Triassic (P-Tr) extinction, marked by high organic matter and sulfur contents, and absence of bioturbation (Piasecki and Stemmerik, 1991; Georgiev et al., 2011). We sampled eleven ~1-cm-thick vertical drill core intervals (core GGU 303102, drilled onshore on a plateau above the valley cut by Triaselv ("Triassic River") of East Greenland, ~20 m total depth). The studied samples belong to two organic-rich shale units recognized within shallow drill core, known as the upper and lower laminated intervals of the Ravnefjeld Formation, respectively (GRL-UL and GRL-LL; Fig. 1). Correlative samples from the Ravnefjeld Formation in GRL were collected from an outcrop in the Triaselv valley on the east side of Schuchert Dal, East Greenland, ~ 6.7 km northwest of the drill core location (Fig. 1). The 29 collected outcrop samples were subdivided into four groups based on their stratigraphic position within the outcrop: GRL-O1-a, GRL-O1-b, GRL-O2-a, and GRL-O2-b. The Lower Turbidite Unit from offshore drill core 6611/09-U-01 in MNS, which penetrates a sandstone- and siltstone-rich turbidite sequence, is considered a stratigraphic equivalent of the Ravnefjeld Formation in GRL in terms of geochemistry and palynology (Bugge et al., 2002; Hochuli et al., 2010). The GRL and MNS depositional localities were close to each other before the opening of the North Atlantic during the Permian-Triassic (Müller et al., 2005). Twenty-four samples from four vertical intervals from the MNS core were studied. From top to bottom, these are the laminated intervals (MNS-UL1, MNS-UL2, and MNS-LL), and the Bottom Shale interval (MNS-BS; Fig. 1). Additional details on the geological setting and samples are provided in Georgiev et al. (2012).

Re-Os dating of GRL and MNS shales using drill core samples yield precise latest Permian ages (253–252 Ma), and Re-Os and other trace element concentration data were used to argue for simultaneous anoxia, temperature increase, and rising acidity (Georgiev et al., 2011). In stark contrast, incipiently weathered black shale from the Ravnefjeld Formation in GRL outcrop showed poor isochroneity (Georgiev et al.,

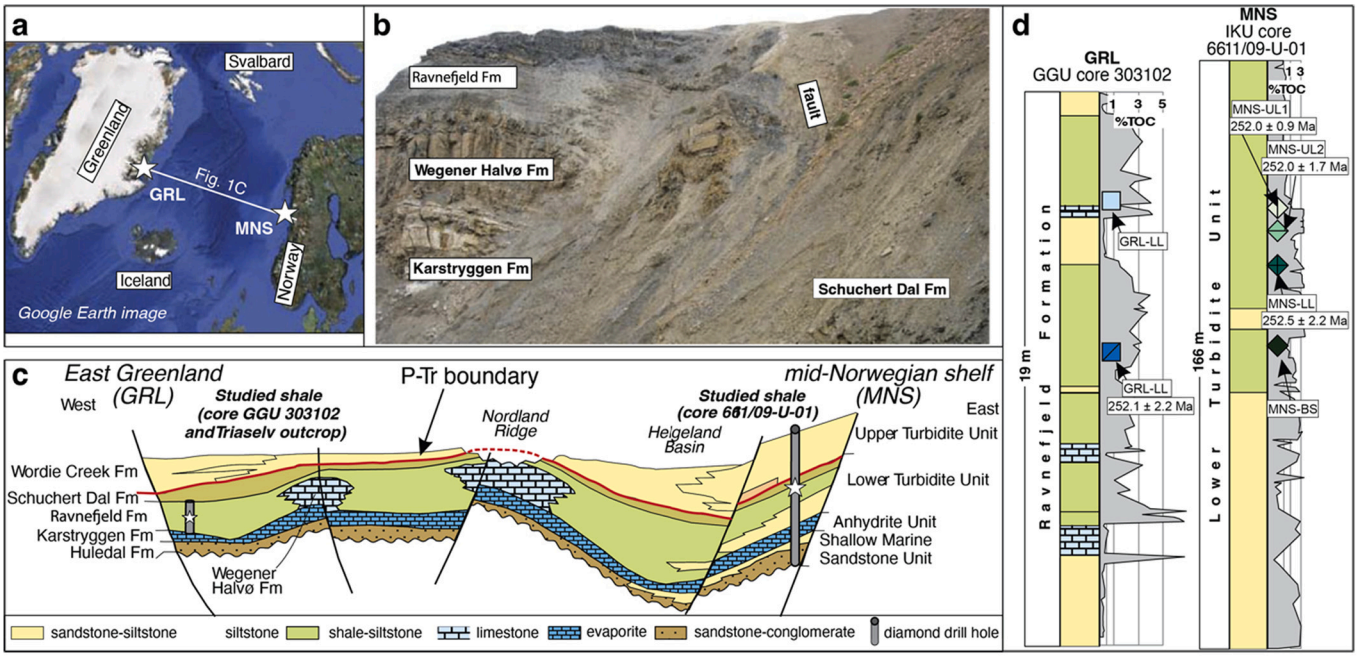

Fig. 1. (a) Locations of the two sections, East Greenland (GRL) and mid-Norwegian shelf (MNS); (b) View of GRL Ravnefjeld Formation shales (upper left); (c) Lithostratigraphic cross-section between GRL and MNS from Upper Permian to Lower Triassic formations. White stars indicate shale sections in this study. (d) Detailed lithostratigraphy and chemostratigraphy of TOC for the Ravnefjeld Formation in GRL and Lower Turbidite Unit in MNS. The six sampled shale intervals are marked with different symbols and abbreviations on their locations with Re-Os ages. Modified from Georgiev et al. (2012).

2012). Further geochemical study of the pristine samples using Cd and N isotopes and trace metal data suggests that the Greenland-Norway seaway, in which GRL and MNS samples were deposited, had strong upwelling and high nutrient utilization (Georgiev et al., 2015).

3. Methods

Shale powders were prepared as part of previous studies (Georgiev et al., 2012). Mercury contents were obtained using the direct mercury analyzer (Milestone© DMA-80 Evo) in the AIRIE Program labs at Colorado State University. About 100 to 250 mg of black shale powder is weighed and transferred into a nickel boat which is autonomously

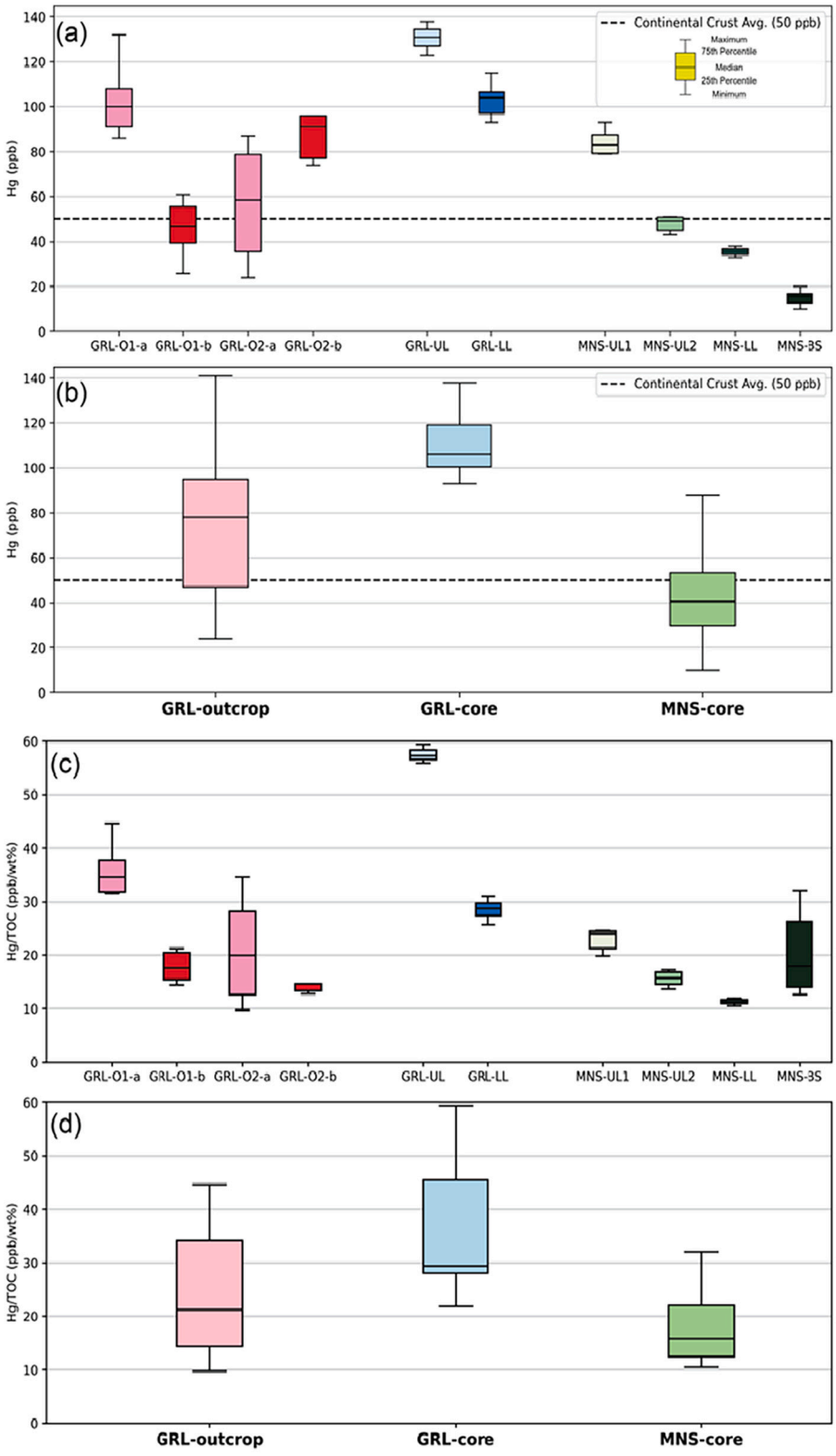

Fig. 2. Box plots of Hg contents from different groups in GRL and MNS. (a) Box plot of all groups in GRL outcrop, GRL core, and MNS core. The GRL samples have higher Hg contents than the MNS samples. MNS-BS has a much lower Hg concentration compared to other groups. Outcrop samples show the highest variability in Hg concentrations. (b) Merged box plot of GRL outcrop, GRL core, and MNS core. Mercury contents of the three groups are statistically different in each group at 95% confidence ($p < 0.01$). The average Hg value of the continental crust of 50 ppb is from Rudnick et al. (2003). (c) and (d) Normalizing Hg to TOC reduces the spread among sample groups; in particular, MNS-BS overlaps all other MNS groups.

loaded into the DMA combustion chamber. The sample undergoes combustion, catalyzation (conversion to native mercury), amalgamation, and spectrophotometry.

Measured mercury intensity is compared to a calibration curve derived from systematic measurements of serial dilutions of a liquid mercury standard (SCP Science AA Standard). Instrument and Ni boat backgrounds are monitored during each run and geological reference materials (SDO-1 and NIST 1632e) are routinely analyzed to track instrument accuracy and precision. The average Hg value of SDO-1 measured here is 7% higher than the expected reference value, which is within the reported uncertainties (Kane, 1993). All measurements are within 10% variance of the average. The average Hg value of NIST 1632e measured here is 4% higher than the expected reference, and all measurements are within 10% variance of the average, excluding a single measurement showing 12% higher Hg content than the average. Table S1 shows the detailed results of standards monitored during measurements. All samples except two with limited powder were measured twice in two duplicate runs; we used the average value of the two duplicate runs as representative Hg contents of these samples (Table S2). Most duplicate runs reproduced within 10%. Duplicates of two samples in MNS-UL1, 241.12–241.14 and 241.19–241.20 are reproducible within 14% and 11%, respectively. Mercury concentration data are discussed together with published geochemical datasets for the same GRL and MNS samples (Georgiev et al., 2011, 2012).

We coded up PCA using Python 3.7 and conducted PCA on two different datasets. The first PCA run focused on drill core samples with 23 chemical variables (Re, Os, Hg, V, Mo, TOC, Ca, Sr, Cu, Cr, Ni, Mn, Zn, Co, S, Sc, Fe, Mg, Al, Rb, Th, P, and Cd contents; Table S3) to identify the difference in sediment inputs. The second PCA run focused on both GRL outcrop and GRL drill core samples with five variables (Hg, S, Sc, Hydrogen Index – HI, and Oxygen Index – OI; Table S4), which are all likely affected by weathering, to verify the behavior of Hg during incipient weathering. Details on PCA are provided in the Supplementary Documentation.

4. Results

All data in this study are available in the supplementary data file (Tables S2, S3, and S4). Mercury contents for the GRL and MNS samples vary between 10 and 144 ppb (Fig. 2a and b), and ratios of Hg/TOC for GRL and MNS samples vary between 10 and 59 (Fig. 2c and d). In MNS shales, Hg contents systematically increase up-section from MNS-BS to MNS-UL1 (15 ppb to 81 ppb on average). In GRL shales, Hg contents are notably higher than for MNS shales, reaching mean values of 110 ppb Hg for GRL drill core samples and 75 ppb Hg for GRL outcrop samples. The Hg/TOC ratios vary similarly to Hg contents, with two distinctions: (1) Hg/TOC ratios in the MNS-BS are higher than Hg/TOC ratios in the remaining, organic-rich MNS-BS units, and (2) the difference between Hg/TOC ratios of GRL core and GRL outcrop samples decreases. Hg contents of MNS core and GRL core samples plotted against TOC, S, Ca, and Al, as proxies for OM, sulfide, carbonate, and clay minerals, respectively, reveal several important features (Fig. 3). The suboxic MNS-BS samples deviate from the trends defined by most other anoxic samples from MNS and GRL, suggesting that the presence of dissolved oxygen in the water column affects Hg speciation. When the MNS-BS samples are excluded, Hg concentrations in all remaining anoxic and euxinic shales show the strongest positive correlation with Ca ($p < 0.01$ and $r = 0.83$, $n = 27$; Fig. 3a), followed by a relatively good positive correlation with TOC ($p < 0.01$ and $r = 0.59$, $n = 24$; Fig. 3b; note that the three GRL-UL samples are excluded from these statistics, as

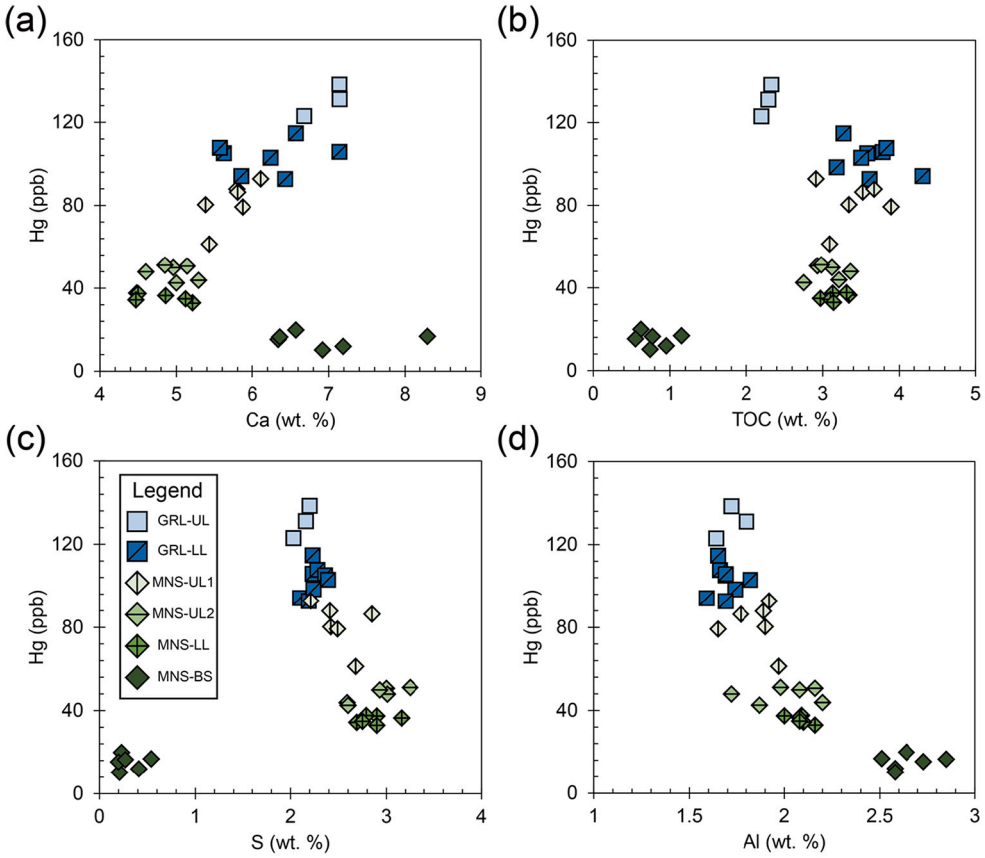

Fig. 3. X-Y plots of Hg versus selected elemental proxies for possible hosts in GRL and MNS core samples – (a) Ca for carbonate, (b) TOC for organic matter, (c) S for sulfide, and (d) Al for clay. Note that MNS-BS is a suboxic shale deposited prior to the overlying anoxic MNS and GRL shales that are characterized by high contents of redox-sensitive metals like Mo, Re, Cd, and Se (Georgiev et al., 2011, 2015).

discussed below). Interestingly, the MNS data generally form curvilinear arrays in Fig. 3, unlike GRL samples that define relatively tight, high Hg clusters.

Results from the first PCA for MNS and GRL core samples are shown in Fig. 4a and b. Most of the elements are bisected by the first principal component (PC 1), which can explain 53% of the elemental distribution (Fig. 4a). PC 1 is ascribed to a contrast between two different element groups: Re, Mo, S, Os, V, and TOC have strong positive signals (>0.5 for PC 1), whereas Al, Rb, Fe, and Th show strong negative signals (<−0.5 for PC 1). The second component, PC 2, explains 21% of the elemental distribution and includes Ca, Mn, and Cr as positive PC 2 and TOC, S, and Fe as negative PC 2. When individual groups of samples are plotted in this two-component space (PC 1 vs. PC 2), GRL and MNS sample groups are clearly separated (Fig. 4b). Outcrop samples from GRL were compared with their equivalent core samples to directly examine weathering effects on Hg concentrations in black shale by the second PCA (Fig. 4c and d). Here, PC 1 explained 72% of the elemental distribution and isolated OI from other variables (Fig. 4c). Outcrop and core shales have distinct PC 1 (Fig. 4d). Only Hg shows a highly negative PC 2 value (−0.75).

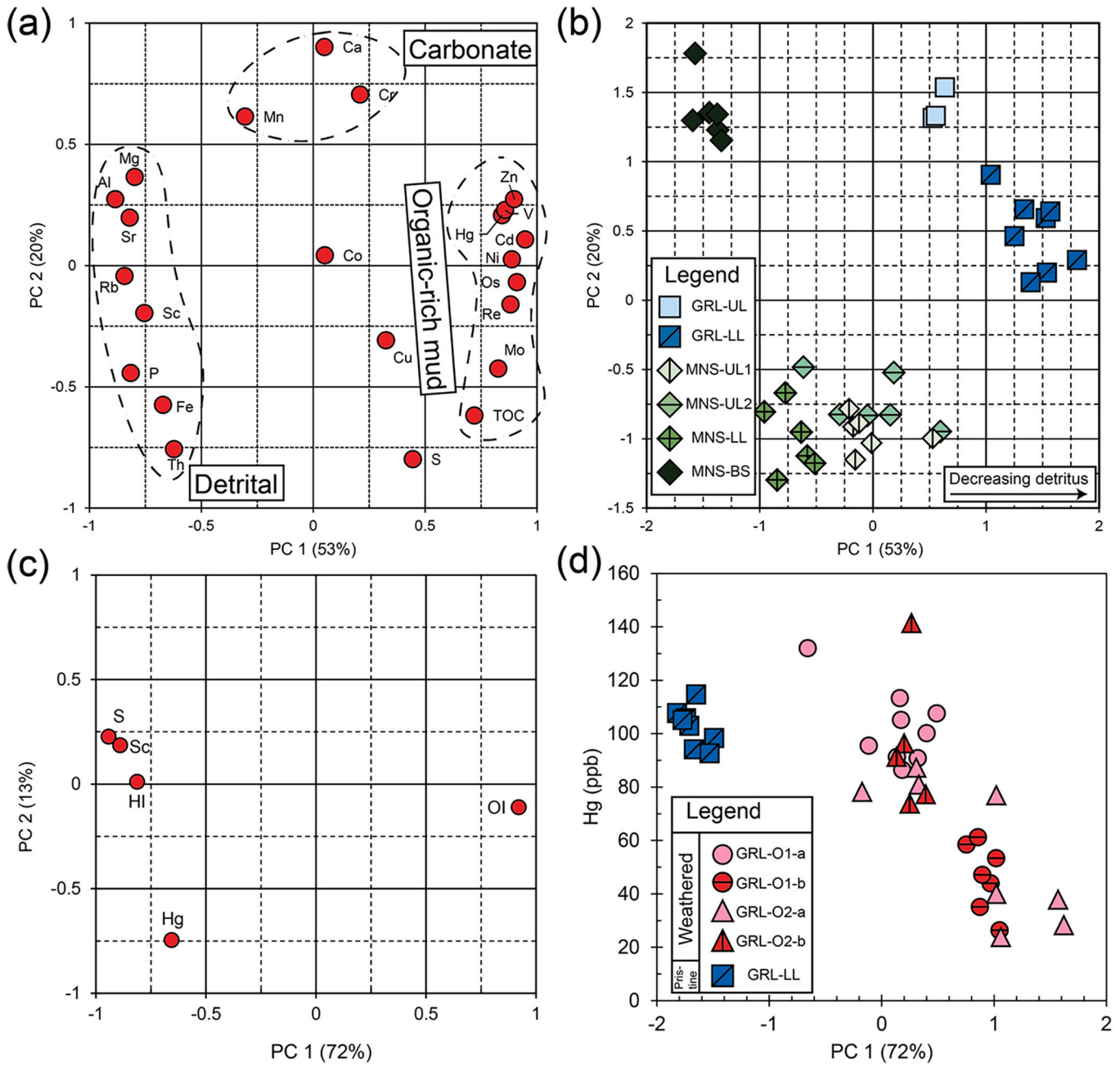

Fig. 4. The results of the first PCA with pristine GRL and MNS drill core samples (a, b) and the second PCA with pristine GRL samples and incipiently weathered GRL outcrop samples (c, d); (a) Principal components (PCs) with major and trace elements; (b) The distribution of core samples by PC 1 and PC 2. GRL and MNS shales are grouped by PC 1 and PC 2, indicating different depositional environments; (c) PC 1 and PC 2 of the second PCA with variables vulnerable to incipient weathering (Note that HI is hydrogen index and OI is oxygen index from Rock-Eval analyses); (d) Hg contents vs. PC 1 of the second PCA, indicating the degree of the weathering. The good correlation between Hg contents and PC 1 indicates that Hg is vulnerable to incipient weathering. Note that GRL-UL unit shows chemical evidence for incipient weathering, whereas all remaining units in GRL core samples are considered pristine and unaffected by weathering (Georgiev et al., 2012).

5. Discussion

5.1. Weathered outcrop and pristine black shale samples

GRL outcrop samples all show poor Re-Os isochroneity, whereas the GRL-LL core produced a precise Re-Os isochron (Georgiev et al., 2011, 2012). Importantly, the GRL outcrop samples do not have significant weathered features such as a yellowish-reddish color; rather, the disturbed Re-Os isotope systematics, the lower S contents compared to correlative GRL core samples, and the higher oxygen indices from Rock-Eval analyses found in GRL outcrop samples mark their state of incipient weathering (Georgiev et al., 2012). The uppermost studied core interval from GRL, GRL-UL, also exhibits geochemical signals indicative of more subtle weathering and produced a disturbed Re-Os isochron (Georgiev et al., 2012). These authors suggested that a notably shallower depth for GRL-UL (~4.5 m) might have put these shales in contact with oxidizing surface water or groundwater, whereas GRL-LL (~10 m depth) was below the reach of oxidizing water. Thus, GRL outcrop shales, and, to a lesser degree, the GRL-UL drill core interval have been affected by oxidation.

The lowermost shale interval in MNS, the MNS-BS, plots away from other drill core shale samples (Figs. 3, 4b). Low concentrations of redox-sensitive trace elements (RSTE: U, V, Se, Re, Os, and Mo) and sulfide-bound trace elements (SBTE: Ni, Zn, Cu, As, Co, and Cd) and low Mo/TOC ratio for MNS-BS shales suggest deposition under more oxygenated conditions, which is also reflected in the larger scatter of the Re-Os isochron data for this interval (MSWD = 14; Georgiev et al., 2011). Here, we focus on estimating Hg behavior in organic-rich black shale during incipient weathering by comparing pristine organic-rich shales with their weathered counterparts (weathered GRL and pristine GRL). As the MNS-BS has no weathered analogue among the studied samples, MNS-BS data are not used to evaluate the effects of weathering. However, all pristine samples, including MNS-BS, are used to evaluate the depositional environment and the hosts of Hg within the GRL-MNS shales.

5.2. Depositional environments and hosts for Hg

GRL drill core shales have twice the average Hg content of MNS drill core shales (Figs. 2, 3), even though shales at both localities are time equivalent, deposited at 252 Ma near each other prior to the opening of the North Atlantic Ocean (Georgiev et al., 2012). When PCA was performed with pristine black shales only (GRL-UL, MNS-UL1, MNS-UL2, MNS-LL, and MNS-BS; Fig. 4a and b), Fig. 4a shows that the majority of the elemental variations (51%) are explained by PC 1 representing authigenic (positive PC 1) and detrital minerals (negative PC 1). Although GRL and MNS Upper Permian shales both reflect anoxic conditions (Georgiev et al., 2012), pristine MNS shales show more detrital input (PC 1 between −1 and + 1) than pristine GRL with PC 1 > 1 (Fig. 4b). The difference in the detrital vs. authigenic phases apparently exerts a primary control of Hg contents in GRL and MNS. This observation is consistent with the interpretation from heavier C isotopes in MNS black shales, suggesting a higher proportion of terrigenous OM compared to GRL black shales (Bugge et al., 2002). Sanei and Goodarzi (2006) pointed out that terrigenous OM is too refractory to concentrate Hg in its structure chemically. Thus, the differences in Hg concentrations between MNS and GRL could be attributable to the changing balance between two distinct sources: the supply of terrigenous materials and the formation of authigenic phases.

The MNS data are aligned along a curvilinear line towards the tight cluster of GRL samples (Fig. 3), suggesting that the depositional environment in MNS gradually evolved towards an environment similar to GRL. Of all MNS samples, the MNS-UL1 shales are most similar to GRL-LL samples in Hg contents (Figs. 2, 3). Our first PCA results show that detrital inputs decrease (PC 1 increases) from MNS-LL towards MNS-UL1 and MNS-UL2 (Fig. 4b), which again suggests that the balance between detrital supply and authigenic precipitation is the major control on Hg content of these shales. Georgiev et al. (2015) argued that the strength of upwelling in MNS was steadily developed from MNS-BS to MNS-LL and MNS-UL, and the upwelling in GRL is stronger than in MNS. Thus, linear arrays of MNS data towards GRL data in Fig. 3 may also reflect this gradual increase of the upwelling strength in MNS.

The main potential hosts for Hg in shale are OM, sulfide, and clay minerals (e.g., Shen et al., 2020), with carbonate minerals representing an additional possibility in modern sediments (Orecchio and Polizzotto, 2013). The inverse relationship between Hg and Al in all studied shales clearly shows that the detrital influx (marked by high Al contents) into the anoxic-euxinic depositional basin dilutes Hg contents (Fig. 3d). Interestingly, Ca contents display the best positive correlation with Hg ($p < 0.01$ and $r = 0.83$; Fig. 3a), suggesting that carbonates may host significant Hg in shales. To assess whether carbonate in MNS shales holds Hg or not, we analyzed the solutions and shale residues following HCl treatment of selected MNS shales. Black shale powders were soaked in 1 mol/L HCl until all CO_2 was degassed. Residual shale was separated from the acidic solution, rinsed with Milli-Q water, and dried. Precipitates of the acidic solution may contain any Hg held by carbonates unless lost during the experiment. We analyzed both the precipitates (to evaluate is Hg was released during carbonate dissolution) and the residual shales (to confirm the extent of Hg removal during carbonate dissolution). The similar contents of original powders and de-carbonized powders (the residual shale after being treated by HCl) show that carbonate does not hold Hg in MNS shale (Fig. 5 and Table S5). Therefore, we exclude clay and carbonate minerals as a significant host for Hg, noting that further research is needed to identify the relationship between Hg and Ca in other settings.

Like Al, S contents also show an inverse correlation with Hg, indicating that sulfide minerals are not the main host of Hg in shale (Fig. 3c), although Shen et al. (2019b) argued that syngenetic pyrite would take in Hg under intensely reduced/euxinic conditions. In contrast, TOC has a positive correlation with Hg in studied shales (Fig. 3b). The coefficient of determination – r value – of the Hg vs. TOC regression ($r = 0.59$) seems too low to firmly establish that OM is the principal host for Hg. However, the correlation is significant based on the p-value ($p < 0.01$). Also, other possible hosts such as clay, carbonate, and sulfide were excluded as

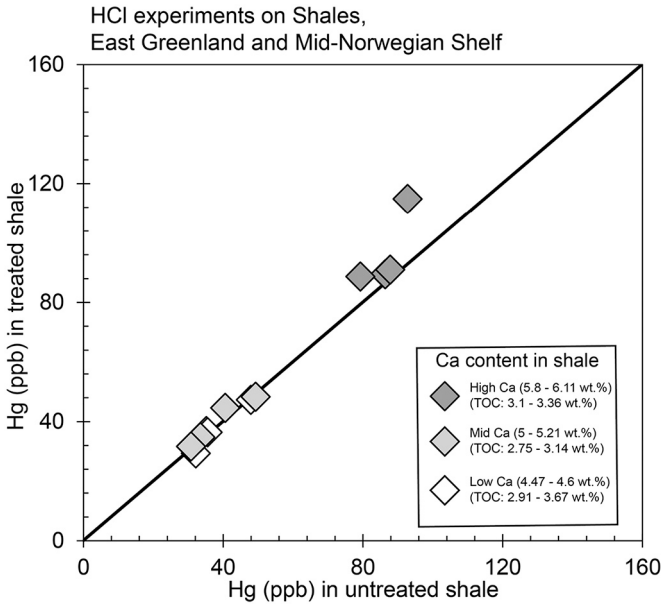

Fig. 5. Hg contents before (x-axis) and after (y-axis) the HCl treatment of shale powders. De-carbonized shales after the HCl treatment have similar contents to original untreated powders, indicating that carbonate is not a significant host of mercury.

significant Hg hosts, as shown above. Collectively, these observations suggest that OM is the significant host of Hg in the studied samples.

The Mo/TOC ratio in shales is often used to estimate the degree of basin restriction during shale deposition, where low ratios imply a more restricted basin, and high ratios imply a less restricted basin (e.g., Algeo and Lyons, 2006). Studied shales in GRL and MNS were deposited in a less restricted basin based on their relatively high Mo/TOC ratio (~16.7) compared with the Black Sea (~ 4.5). However, the GRL-MNS basin was more restricted than the present-day Saanich Inlet (Mo/TOC of ~45), indicating moderate water restriction for GRL-MNS (Georgiev et al., 2011). Also, the high TOC contents of studied organic-rich shales resulted from a high paleoproductivity caused by intense upwelling (Georgiev et al., 2015). The high correlation between TOC and Hg contents, high paleoproductivity by upwelling, and moderate restriction with limited dissolved oxygen supplies might cause OM to be the principal host of Hg in the Late Permian MNS-GRL basins (see also additional discussion in the supplementary document).

5.3. Effects of incipient weathering on Hg contents

In the second PCA, based on weathered and unweathered GRL samples only (Fig. 4c and d), negative values of PC 1 are related to higher HI and S, Sc, and Hg contents, which collectively indicate weaker weathering or no weathering. In contrast, positive values of PC 1 related to higher OI indicate stronger weathering (Fig. 4c). Hydrogen index is a proxy of the hydrogen content of kerogen, and OI is for the oxygen content (Peters, 1986). These results are consistent with the conclusions of previous studies that show HI decreases and OI increases in black shales during post-depositional processes such as oxidation or maturation (Vandenbroucke and Largeau, 2007; Georgiev et al., 2012; Marynowski et al., 2017; Charbonnier et al., 2020). As a result, PC 1 in the second PCA can be used as a reliable indicator for the degree of weathering in outcrop-derived shale samples (Fig. 4d). Of the five key parameters defining PC 1, only Hg shows a notable (negative) relation to PC 2, which is mainly determined by various Hg contents from GRL samples. PC 2 accounts for only 13% of the elemental distribution, which is much less significant than PC 1 (72%).

The weathering indicator PC 1 shows a significant correlation with Hg in weathered shales ($r = 0.81$, $p < 0.01$). The average TOC content in weathered GRL shales is 9% lower than in pristine GRL (3.28 wt% vs. 3.63 wt%, respectively). However, outcrop shales lost up to 77% of Hg during incipient weathering from an average of 103 ppb Hg in the pristine samples down to a low of 24 ppb Hg in weathered samples (Fig. 4d). The ratios of Hg/TOC in outcrop shales also show up to 64% lower values compared to pristine samples (from 28 down to 10; Fig. S3a). Similar decreasing trends are shown in variations of other weathering vulnerable elements (Mo and Re) with PC 1 of the second PCA (Fig. S2).

Three possible processes might explain the OM-hosted Hg loss during incipient weathering. First, partial degradation of OM, which causes minimal to small TOC loss, could play a critical role in Hg retention during incipient weathering if Hg-rich entities are degraded. Mercury data on modern sediment from eutrophic lakes indicate that soluble organic matter (SOM; the easily degradable lipid fraction) concentrates Hg and other OM-related metals, even as SOM accounts for 2.5 wt% of the whole rock on average (Sanei and Goodarzi, 2006). In addition, transformations of the kerogen and SOM structure by the oxidation process may release Hg hosted by OM. Low molecular weight organic compounds like methylnaphthalenes, dibenzofuran, or dibenzothiophene are susceptible even during incipient weathering (Marynowski et al., 2011), and some of these may account for part of the Hg loss. Loss of Mo and altered Mo stable isotope ratios were also reported from partially weathered black shales (Marynowski et al., 2017). In addition, destruction of specific components in kerogen that may preferentially hold Hg may play the main role in releasing Hg. Preferential destruction of aliphatic kerogen compared to carbonyl and aromatic components during weathering has been reported, although the degree of weathering of the studied samples was higher than incipient weathering (Petsch et al., 2001). Thus, Hg loss in samples during incipient weathering could be caused by partial degradation or transformations of OM. In our study, sulfide oxidation is unlikely to be the main reduction process for Hg in the studied shales because sulfide is not a primary host of Hg in pristine samples (Fig. 2c). In sedimentary rocks with sulfide-hosted Hg, the Hg concentrations will be more vulnerable to incipient weathering because oxidation of sulfide is faster and occurs earlier than that of OM (Petsch et al., 2000; Wildman et al., 2004; Georgiev et al., 2012; Marynowski et al., 2017).

Our results show that incipient weathering may dampen and conceal originally higher Hg and Hg/TOC ratios in sedimentary rocks (Fig. 4d and S2a). Peaks of Hg signals in sediments have been highlighted as a LIP tracer for decades, but concealed Hg signals in sedimentary sections came to be highlighted recently. For example, the Toarcian Oceanic Anoxic Event (T-OAE; ~183 Ma) is a well-studied anoxic event that was probably caused by eruptions of the Karoo-Ferrar LIP (e.g., Percival et al., 2015). Elevated Hg contents and Hg/TOC ratios would be expected in Toarcian sediments, but some T-OAE sections do not show Hg anomalies (Them et al., 2019). The authors ruled out the possibility of diagenesis (including weathering) to explain the lack of Hg/TOC signals because they assumed that Hg is mainly hosted by OM (Them et al., 2019). Nonetheless, results in this study, in which TOC (representing OM) and Hg are impacted at different stages of weathering, suggest that dampened Hg/TOC signals may be caused by incipient weathering. Also, the magnitude of Hg/TOC peaks in some ancient organic-rich shales may depend on how euxinic the depositional environment is (Shen et al., 2020). Under strongly euxinic conditions, sulfide is a more prominent host for Hg, and incipient weathering may indeed affect sulfide-hosted Hg concentrations more profoundly than our samples, in which Hg is mainly hosted by OM.

Overall, we suggest a schematic diagram of Hg, S, TOC, and Hg/TOC changes with the degree of weathering (Fig. 6). The ratio is established at a certain point when the rock is pristine. During incipient weathering, TOC and Hg content decrease with different slopes while S content decreases severely. As a result, the Hg/TOC ratio decreases, even though TOC content remains relatively constant. During extreme weathering, loss of TOC is dramatic, and the Hg/TOC ratio may increase sharply as TOC contents decrease to 1% or less (Charbonnier et al., 2020). Thus, incipient weathering may release Hg, masking possible positive Hg anomalies even as TOC contents remain constant. Extreme weathering, in contrast, can degrade organic matter, resulting in loss of TOC and an increase in Hg/TOC, potentially misinterpreted as a positive Hg anomaly. Given these results, caution is necessary for the interpretation of Hg

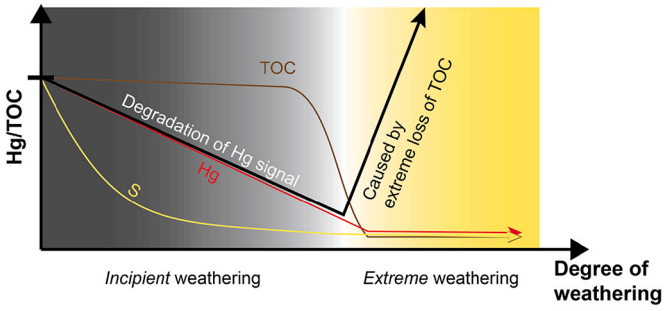

Fig. 6. Schematic illustration of Hg/TOC ratio, TOC, Hg, and S changes in organic-rich shales during weathering. Degradation of Hg signals occurs even with incipient and invisible weathering, while degradation of OM is limited as shown in this study. This lowers the Hg/TOC ratio, a parameter in use to characterize paleo-environments. In contrast, loss of organic matter during extreme weathering dramatically increases Hg/TOC ratios (Charbonnier et al., 2020). The loss of S proceeds OM loss (Petsch et al., 2000; Georgiev et al., 2012).

concentrations and Hg/TOC ratios, particularly when positive anomalies are expected, but not observed, even if the shales look fresh and TOC values do not seem to be strongly reduced by weathering.

6. Conclusion

Detailed analysis of mercury contents using statistical tools and an expanded geochemical dataset from previous studies of GRL and MNS Upper Permian shales clarify the effect of incipient weathering on shale Hg contents. Mercury contents from the GRL and MNS drill cores average 110 ppb and 55 ppb, respectively; the difference between the two sites is attributed to the degree of detrital influx, including kerogen types (OM sources). A detailed comparison between Hg and possible host elements demonstrates that organic matter is the main Hg host in Upper Permian shales from GRL and MNS drill cores. Those shales were deposited in a setting with a high paleoproductivity by upwelling and moderate basin restriction. Up to 77% Hg loss and up to 64% lower Hg/TOC ratios were observed in incipiently weathered GRL outcrop shales that appear visually fresh (based on Re-Os isotopic characteristics and other chemical criteria). Destruction of soluble organic matter or specific kerogen entities and transformation of kerogen components are the likely causes of lower Hg contents of partly weathered samples, although further research is needed to constrain the exact cause. The observed Hg loss upon incipient weathering calls for prudent interpretations of Hg data in outcrop shales. Identification of weathering is an essential prerequisite that needs to be applied prior to interpretations of paleoenvironmental conditions based on the Hg geochemistry of outcrop samples.

Declaration of Competing Interest

The authors declare that they have no known competing financial interests or personal relationships that could have appeared to influence the work reported in this paper.

Acknowledgments

We thank Stefan Piasecki (GEUS) for providing Greenland cores and the late Hermann Weiss (SINTEF) for access to IKU mid-Norwegian shelf cores. CSU provides no salary support for the AIRIE Program or for operation of the AIRIE Re-Os Laboratory Facility. JP thanks Aaron Zimmerman and Gang Yang for their help in the AIRIE Labs. JP was supported on an American Chemical Society grant (PRF# 59965-ND2) to HS. Open access to this article was made possible by CSU Libraries Open Access Research and Scholarship Fund (OARS). Beginning in February 2022, SVG is supported by the Bulgarian National Science Fund grant КП-06-ДВ/6.

Appendix A. Supplementary data

Supplementary data to this article can be found online at https://doi.org/10.1016/j.chemgeo.2022.121030.

References

Algeo, T.J., Lyons, T.W., 2006. Mo–total organic carbon covariation in modern anoxic marine environments: Implications for analysis of paleoredox and paleohydrographic conditions. Paleoceanography 21 (1). https://doi.org/10.1029/2004PA001112.

Bugge, T., Ringas, J.E., Leith, D.A., Mangerud, G., Weiss, H.M., Leith, T.L., 2002. Upper Permian as a new play model on the mid-Norwegian continental shelf: Investigated by shallow stratigraphic drilling. AAPG Bull. 86 (1), 107–127. https://doi.org/10.1306/61eeda4e-173e-11d7-8645000102c1865d.

Charbonnier, G., Adatte, T., Föllmi, K.B., Suan, G., 2020. Effect of intense weathering and postdepositional degradation of organic matter on Hg/TOC proxy in organic-rich sediments and its implications for deep-time investigations. Geochem. Geophys. Geosyst. 21 (2) https://doi.org/10.1029/2019GC008707.

Clapham, M.E., Renne, P.R., 2019. Flood Basalts and Mass Extinctions. Annu. Rev. Earth Planet. Sci. 47 (1), 275–303. https://doi.org/10.1146/annurev-earth-053018-060136.

Fitzgerald, W., Lyons, W., 1973. Organic mercury compounds in coastal waters. Nature 242, 452–453. https://doi.org/10.1038/242452a0.

Gehrke, G.E., Blum, J.D., Meyers, P.A., 2009. The geochemical behavior and isotopic composition of Hg in a mid-Pleistocene western Mediterranean sapropel. Geochim. Cosmochim. Acta 73 (6), 1651–1665. https://doi.org/10.1016/j.gca.2008.12.012.

Georgiev, S., Stein, H.J., Hannah, J.L., Bingen, B., Weiss, H.M., Piasecki, S., 2011. Hot acidic late Permian seas stifle life in record time. Earth Planet. Sci. Lett. 310 (3–4), 389–400. https://doi.org/10.1016/j.epsl.2011.08.010.

Georgiev, S., Stein, H.J., Hannah, J.L., Weiss, H.M., Bingen, B., Xu, G., Rein, E., Hatlø, V., Løseth, H., Nali, M., Piasecki, S., 2012. Chemical signals for oxidative weathering predict Re-Os isochroneity in black shales, East Greenland. Chem. Geol. 324–325, 108–121. https://doi.org/10.1016/j.chemgeo.2012.01.003.

Georgiev, S.V., Horner, T.J., Stein, H.J., Hannah, J.L., Bingen, B., Rehkämper, M., 2015. Cadmium-isotopic evidence for increasing primary productivity during the late Permian anoxic event. Earth Planet. Sci. Lett. 410, 84–96. https://doi.org/10.1016/j.epsl.2014.11.010.

Hochuli, P.A., Vigran, J.O., Hermann, E., Bucher, H., 2010. Multiple climatic changes around the Permian-Triassic boundary event revealed by an expanded palynological record from mid-Norway. Bull. Geol. Soc. Am. 122 (5–6), 884–896. https://doi.org/10.1130/B26551.1.

Kane, J.S., 1993. USGS Reference Sample Devonian Ohio Shale SDO-1. U.S. Geological Survey.

Kongchum, M., Hudnall, W.H., Delaune, R.D., 2011. Relationship between sediment clay minerals and total mercury. J. Environ. Sci. Health A 46 (5), 534–539. https://doi.org/10.1080/10934529.2011.551745.

Marynowski, L., Kurkiewicz, S., Rakociński, M., Simoneit, B.R., 2011. Effects of weathering on organic matter: I. changes in molecular composition of extractable organic compounds caused by paleoweathering of a lower Carboniferous (Tournaisian) marine black shale. Chem. Geol. 285 (1–4), 144–156. https://doi.org/10.1016/j.chemgeo.2011.04.001.

Marynowski, L., Pisarzowska, A., Derkowski, A., Rakociński, M., Szaniawski, R., Środoń, J., Cohen, A.S., 2017. Influence of palaeoweathering on trace metal concentrations and environmental proxies in black shales. Palaeogeogr. Palaeoclimatol. Palaeoecol. 472, 177–191. https://doi.org/10.1016/j.palaeo.2017.02.023.

Müller, R., Nystuen, P.J., Eide, F., Lie, H., 2005. Late Permian to Triassic basin infill history and palaeogeography of the Mid-Norwegian shelf-East Greenland region. Norwegian Petrol. Soc. Spec. Publ. 12 (C), 165–189. https://doi.org/10.1016/S0928-8937(05)80048-7.

Orecchio, S., Polizzotto, G., 2013. Fractionation of mercury in sediments during draining of Augusta (Italy) coastal area by modified Tessier method. Microchem. J. 110, 452–457. https://doi.org/10.1016/j.microc.2013.05.015.

Peng, B., Song, Z., Tu, X., Xiao, M., Wu, F., Lv, H., 2004. Release of heavy metals during weathering of the lower Cambrian Black Shales in western Hunan, China. Environ. Geol. 45 (8), 1137–1147. https://doi.org/10.1007/s00254-004-0974-7.

Percival, L.M.E., Witt, M.L.I., Mather, T.A., Hermoso, M., Jenkyns, H.C., Hesselbo, S.P., Al-Suwaidi, A.H., Storm, M.S., Xu, W., Ruhl, M., 2015. Globally enhanced mercury deposition during the end-Pliensbachian extinction and Toarcian OAE: a link to the Karoo-Ferrar Large Igneous Province. Earth Planet. Sci. Lett. 428, 267–280. https://doi.org/10.1016/j.epsl.2015.06.064.

Percival, L.M.E., Jenkyns, H.C., Mather, T.A., Dickson, A.J., Batenburg, S.J., Ruhl, M., Hesselbo, S.P., Barclay, R., Jarvis, I., Robinson, S.A., Woelders, L., 2018. Does large igneous province volcanism always perturb the mercury cycle? Comparing the records of Oceanic Anoxic event 2 and the End-cretaceous to other Mesozoic events. Am. J. Sci. 318 (8), 799–860. https://doi.org/10.2475/08.2018.01.

Peters, K.E., 1986. Guidelines for Evaluating Petroleum Source Rock Using Programmed Pyrolysis. AAPG Bulletin 70 (3), 318–329.

Petsch, S.T., Berner, R.A., Eglinton, T.I., 2000. A field study of the chemical weathering of ancient sedimentary organic matter. Org. Geochem. 31 (5), 475–487. https://doi.org/10.1016/S0146-6380(00)00014-0.

Petsch, S.T., Smernik, R.J., Eglinton, T.I., Oades, J.M., 2001. A solid state 13C-NMR study of kerogen degradation during black shale weathering. Geochim. Cosmochim. Acta 65 (12), 1867–1882. https://doi.org/10.1016/S0016-7037(01)00572-5.

Piasecki, S., Stemmerik, L., 1991. Late Permian anoxia in central East Greenland. Geol. Soc. Spec. Publ. 58 (58), 275–290. https://doi.org/10.1144/GSL.SP.1991.058.01.18.

Rudnick, R.L., Gao, S., Holland, H.D., Turekian, K.K., 2003. Composition of the continental crust. Crust 3, 1–64.

Sanei, H., Goodarzi, F., 2006. Relationship between organic matter and mercury in recent lake sediment: the physical-geochemical aspects. Appl. Geochem. 21 (11), 1900–1912. https://doi.org/10.1016/j.apgeochem.2006.08.015.

Shen, J., Chen, J., Algeo, T.J., Yuan, S., Feng, Q., Yu, J., Zhou, L., O'Connell, B., Planavsky, N.J., 2019a. Evidence for a prolonged Permian–Triassic extinction interval from global marine mercury records. Nat. Commun. 10 (1), 1–9. https://doi.org/10.1038/s41467-019-09620-0.

Shen, J., Algeo, T.J., Chen, J., Planavsky, N.J., Feng, Q., Yu, J., Liu, J., 2019b. Mercury in marine Ordovician/Silurian boundary sections of South China is sulfide-hosted and non-volcanic in origin. Earth Planet. Sci. Lett. 511, 130–140. https://doi.org/10.1016/j.epsl.2019.01.028.

Shen, J., Feng, Q., Algeo, T.J., Liu, J., Zhou, C., Wei, W., Liu, J., Them, T.R., Gill, B.C., Chen, J., 2020. Sedimentary host phases of mercury (Hg) and implications for use of Hg as a volcanic proxy. Earth Planet. Sci. Lett. 543 https://doi.org/10.1016/j.epsl.2020.116333.

Them, T.R., Jagoe, C.H., Caruthers, A.H., Gill, B.C., Grasby, S.E., Gröcke, D.R., Yin, R., Owens, J.D., 2019. Terrestrial sources as the primary delivery mechanism of mercury to the oceans across the Toarcian Oceanic Anoxic Event (early Jurassic). Earth Planet. Sci. Lett. 507, 62–72. https://doi.org/10.1016/j.epsl.2018.11.029.

Tuttle, M.L.W., Fahy, J.W., Elliott, J.G., Grauch, R.I., Stillings, L.L., 2014. Contaminants from cretaceous black shale: I. Natural weathering processes controlling contaminant cycling in Mancos Shale, southwestern United States, with emphasis on salinity and selenium. Appl. Geochem. 46, 57–71. https://doi.org/10.1016/j.apgeochem.2013.12.010.

Vandenbroucke, M., Largeau, C., 2007. Kerogen origin, evolution and structure. Org. Geochem. 38 (5), 719–833. https://doi.org/10.1016/j.orggeochem.2007.01.001.

Wildman, R.A., Berner, R.A., Petsch, S.T., Bolton, E.W., Eckert, J.O., Mok, U., Evans, J.B., 2004. The weathering of sedimentary organic matter as a control on atmospheric O2: I. Analysis of a black shale. Am. J. Sci. 304 (3), 234–249. https://doi.org/10.2475/ajs.304.3.234.